NeuroMolecular Medicine (2025) 27:18
https://doi.org/10.1007/s12017-025-08840-6

RESEARCH

NOTCH3 Variant Position Affects the Phenotype at the Pluripotent Stem Cell Level in CADASIL

Ana Bugallo-Casal[1,2] · Elena Muiño[3,4] · Susana B. Bravo[5] · Pablo Hervella[6] · Susana Arias-Rivas[7] · Manuel Rodríguez-Yáñez[7] · Enrique Vara-León[12] · Rita Quintas-Rey[8] · Lara Pérez-Gayol[1] · Olga Maisterra-Santos[9] · Jesús Pizarro-Gonzálvez[9] · María Rosa Martorell-Riera[10] · Cristòfol Vives-Bauzá[11] · Israel Fernández-Cadenas[3] · José Castillo[6] · Francisco Campos[1]

Received: 26 November 2024 / Accepted: 15 February 2025

Abstract

Cerebral autosomal dominant arteriopathy with subcortical infarcts and leukoencephalopathy (CADASIL) is the most common genetic form of stroke. It is caused by a cysteine-altering variant in one of the 34 epidermal growth factor-like repeat (EGFr) domains of Notch3. *NOTCH3* pathogenic variants in EGFr 1–6 are associated with high disease severity, whereas those in EGFr 7–34 are associated with late stroke onset and increased survival. However, whether and how the position of the *NOTCH3* variant directly affects the disease severity remains unclear. In this study, we aimed to generate human-induced pluripotent stem cells (hiPSCs) from patients with CADASIL with EGFr 1–6 and 7–34 pathogenic variants to evaluate whether the *NOTCH3* position affects the cell phenotype and protein profile of the generated hiPSCs lines. Six hiPSCs lines were generated: two from patients with CADASIL with EGFr 1–6 pathogenic variants, two from patients with EGFr 7–34 variants, and two from controls. Notch3 aggregation and protein profiles were tested in the established six hiPSCs lines. Cell analysis revealed that the *NOTCH3* variants did not limit the cell reprogramming efficiency. However, EGFr 1–6 variant position was associated with increased accumulation of Notch3 protein in pluripotent stem cells and proteomic changes related with cytoplasmic reorganization mechanisms. In conclusion, our analysis of hiPSCs derived from patients with CADASIL support the clinical association between the *NOTCH3* variant position and severity of CADASIL.

Keywords CADASIL · Human iPSCs · Disease modeling · *NOTCH3* variant position · Proteomic analysis · Stem cells

✉ Francisco Campos
francisco.campos.perez@sergas.es

[1] Translational Stroke Laboratory Group (TREAT), Clinical Neurosciences Research Laboratory (LINC), Health Research Institute of Santiago de Compostela (IDIS), 15706 Santiago de Compostela, Spain

[2] University of Santiago de Compostela (USC), 15705 Santiago de Compostela, Spain

[3] Stroke Pharmacogenomics and Genetics, Sant Pau Institute of Research (IR Sant Pau), 08041 Barcelona, Spain

[4] Epilepsy Unit, Hospital de la Santa Creu i Sant Pau, 08025 Barcelona, Spain

[5] Proteomic Unit, Health Research Institute of Santiago de Compostela (IDIS), 15706 Santiago de Compostela, Spain

[6] Neuroimaging and Biotechnology Laboratory Group (NOBEL), Clinical Neurosciences Research Laboratory (LINC), Health Research Institute of Santiago de Compostela (IDIS), 15706 Santiago de Compostela, Spain

[7] Stroke Unit, Department of Neurology, Hospital Clínico Universitario, 15706 Santiago de Compostela, Spain

[8] Galician Public Foundation of Genomic Medicine, Genomics Medicine Group, Genetic Group, Health Research Institute of Santiago de Compostela (IDIS), 15706 Santiago de Compostela, Spain

[9] Unidad de Memoria y Demencias, Hospital Universitario Vall d'Hebron/Vall d'Hebron Institut de Reçerca, 08035 Barcelona, Spain

[10] Unidad de Diagnóstico Molecular y Genética Clínica, Hospital Universitari Son Espases, 07120 Palma, Spain

[11] Research Unit, Hospital Universitari Son Espases, IdISBa, Department of Biology, University of Balearic Islands (UIB), IUNICS, 07120 Palma, Spain

[12] Galician Public Foundation of Genomic Medicine, Genomics Medicine Group, 15706, Santiago de Compostela, Spain

Published online: 27 February 2025

Introduction

Cerebral autosomal dominant arteriopathy with subcortical infarcts and leukoencephalopathy (CADASIL) is a rare and severe cerebrovascular disease associated with *NOTCH3* gene mutations. It is characterized by extensive white matter hyperintensities (WMHs), recurrent small deep cerebral infarcts, cognitive decline, motor disability, and psychiatric impairment (Chabriat et al., 1995, 2009; Joutel et al., 1996, 1997; Tournier-Lasserve et al., 1993).

Notch3 is expressed predominantly on the surface of pericytes and vascular smooth muscle cells (VSMCs) in the wall of microvessels (Brulin et al., 2002; Tikka et al., 2009). It acts as a single-pass transmembrane receptor that undergoes proteolytic cleavage upon activation, releasing the Notch intracellular domain (NICD) into the cell for signal transduction and shedding the Notch extracellular domain (NECD) from the cell surface. NECD contains a large sequence of 34 epidermal growth factor-like repeat (EGFr) domains, each with six conserved cysteines. *NOTCH3* mutations result in an uneven number of cysteine residues (gain or loss) in one of the 34 EGFrs of the NECD (Joutel et al., 1996, 1997; Tournier-Lasserve et al., 1993). This results in the multimerization and aggregation of Notch3, observable as intra and extracellular deposits, known as granular osmiophilic material (GOM), via electron microscopy (Monet-Lepretre et al., 2013). Formation of GOM is the main etiopathogenic cause of CADASIL that is histologically correlated with the loss of endothelial and mural cells (VSMCs and pericytes), ultimately leading to vasoreactivity and cerebral hypoperfusion (Gravesteijn et al., 2020).

Location of mutations in *NOTCH3* EGFr domains are associated with the disease severity (Gravesteijn et al., 2022; Hack et al., 2020, 2022, 2023). Cysteine mutations in EGFr domains 1–6 are associated with more severe clinical and imaging features and higher Notch3 accumulation in the vascular wall compared to those in EGFr domains 7–34 (Cho et al., 2021; Gravesteijn et al., 2022; Rutten et al., 2019). This explains the unexpectedly high prevalence of *NOTCH3* mutations in EGFr domains 7–34 in large asymptomatic population-based DNA biobanks (Cho et al., 2021, 2022; Rutten et al., 2019). However, despite the presence of same mutations, most phenotypic variability in CADASIL remains ambiguous (Zhang et al., 2022), with various factors, such as gender (Gunda et al., 2012) and vascular risk factors (Singhal et al., 2004), mediating its severity. Therefore, whether the *NOTCH3* variant position directly affects CADASIL severity remains unclear.

Human-induced pluripotent stem cells (hiPSCs) directly derived from affected patients are extensively used as humanized models to explore the molecular mechanisms related to pathology, identify the biomarkers of disease progression, and develop novel therapies (Ahn et al., 2024; Chen et al., 2020; Fernandez-Susavila et al., 2018; Jalil et al., 2021; Kelleher et al., 2019; Ling et al., 2019; Manini & Pantoni, 2021; Wang et al., 2024; Yamamoto et al., 2020; Zhang et al., 2023).

Using this experiment cell approach, in this study, we aimed to generate hiPSCs from patients with CADASIL with EGFr 1–6 and 7–34 pathogenic variants and controls to evaluate whether the *NOTCH3* variant position affects the phenotypes and protein profiles of the generated hiPSCs lines (Tables 1 and 2).

Results

Clinical Characteristics of Patients with CADASIL

Four patients with CADASIL, including two (one male and one female) with EGFr 1–6 and two (one male and one female) with EGFr 7–34 *NOTCH3* variants, were included in this study. The main clinical and epidemiological characteristics and genetic information of the patients are presented in Table 1A. Magnetic resonance imaging (MRI) scans of the patients used for pathological diagnosis are shown in Fig. 1. Patients with EGFr 1–6 pathogenic variants exhibited symptomatic ischemic stroke, extensive WMHs, multiple lacunes, and microbleeds on the MRI scan. Notably, none of the patients with EGFr 7–34 pathogenic variants exhibited stroke and lacunes on the MRI scan. Additionally, two

Table 2 Characteristics of control subjects

hiPSCs identity	Gender	Ethnicity	Age
CSU	F	Caucasian	30
CSP	M	Caucasian	27

Table 1 Characteristics of CADASIL patients participating in the study

hiPSCs identity	Gender	Ethnicity	Age	Genotype of locus	Exon	Disease
CAD21	F	Caucasian	59	R90C	3	CADASIL
CAD23	M	Caucasian	44	R182C	4	CADASIL
CAD26	M	Caucasian	32	R1242C	23	CADASIL
CAD28	F	Caucasian	64	C591R	1	CADASIL

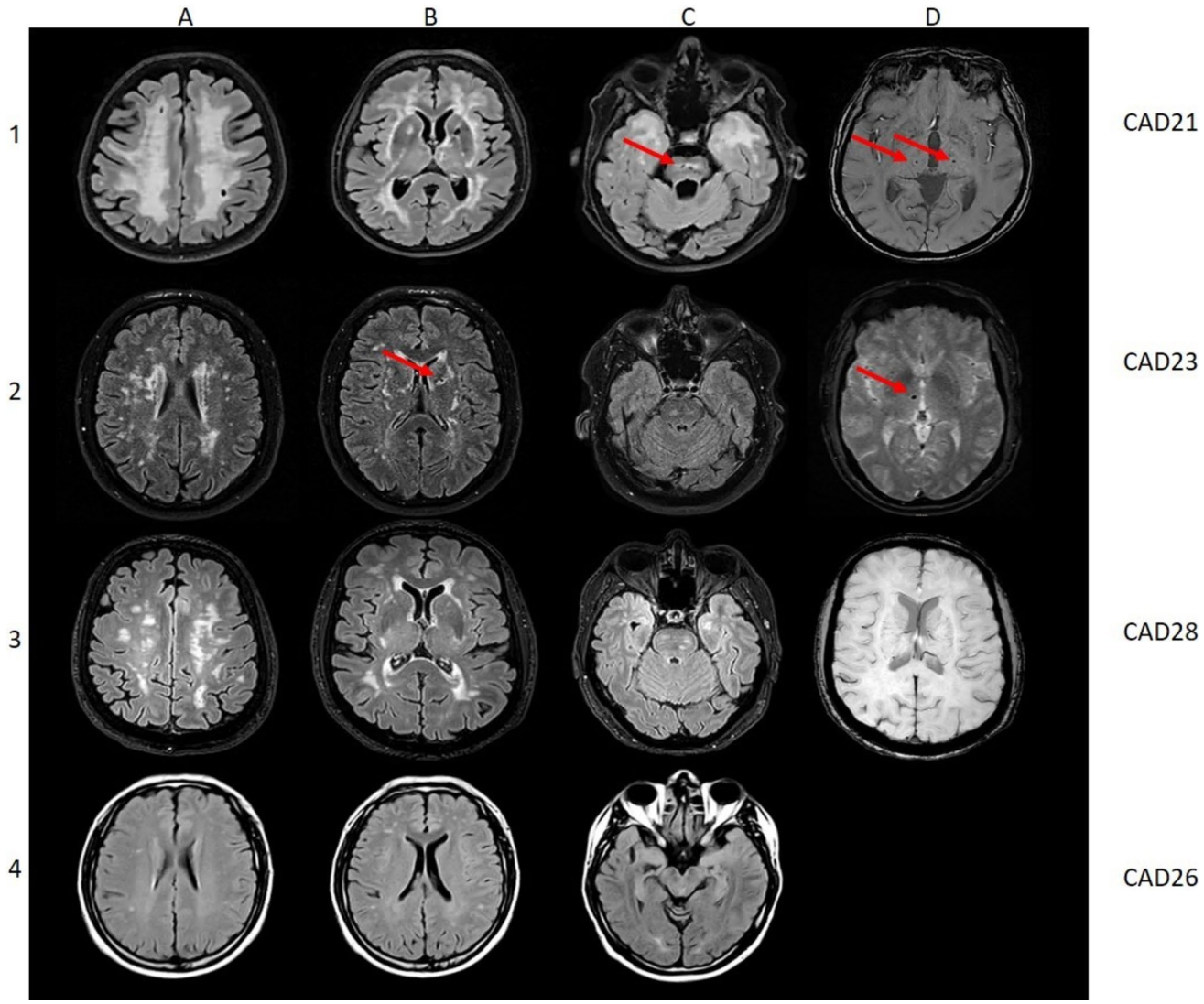

Fig. 1 Cerebral magnetic resonance imaging (MRI) of included CADASIL patients. Panels in the rows A–C show fluid attenuated inversion recovery (FLAIR) images and panels in the row D show susceptibility weighted imaging (SWI). Patients coded as CAD21, CAD23 and CAD28 are patients from Hospital Universitario Vall d´Hebron (Barcelona) and CAD26 is from Hospital Clínico Universitario (Santiago de Compostela). Patient CAD21 (p.R90C) is a 63-year-old woman. In this patient, FLAIR images show extensive and confluent white matter hyperintensities (WMHs) together with multiple lacunes in the basal ganglia, midbrain and pons (marked with a red arrow). On SWI, the patient had multiple microbleeds predominantly in the basal ganglia, temporal, midbrain and infratentorial areas. Two of them are shown in the figure (red arrows). Patient CAD23 is a 44-year-old man (p.R182C). FLAIR images show WMHs and lacunes (one of which is marked with a red arrow) in the basal ganglia, thalamus and corona radiata. SWI showed a microbleed in the left peduncle and another in the right thalamus, which is the one shown in the image (red arrow). Patient CAD28 is a 64-year-old woman (p.C591R). FLAIR images show WMHs but no lacunes. There is no evidence of microbleeds on SWI. The last patient CAD26 is a 32-year-old man (p.R1242C). FLAIR images show very little WMHs. SWI is not available in this patient

controls (one male and one female; Table 1B) were included in the study for comparative analysis.

Characterization of hiPSCs Derived from Healthy Donors and Patients with CADASIL

According to the well-established guidelines for the generation of hiPSCs from human cells (MacArthur et al., 2019), six cell lines (four from patients with CADASIL and two from healthy donors) were generated and characterized by testing the main parameters related to the success of the reprogramming process from the somatic peripheral blood mononuclear cells (PBMCs), to pluripotent state. Karyotype analyses confirmed that the reprogramming procedure did not alter the number and structure of chromosomes in hiPSCs derived from both the healthy donors and patients with

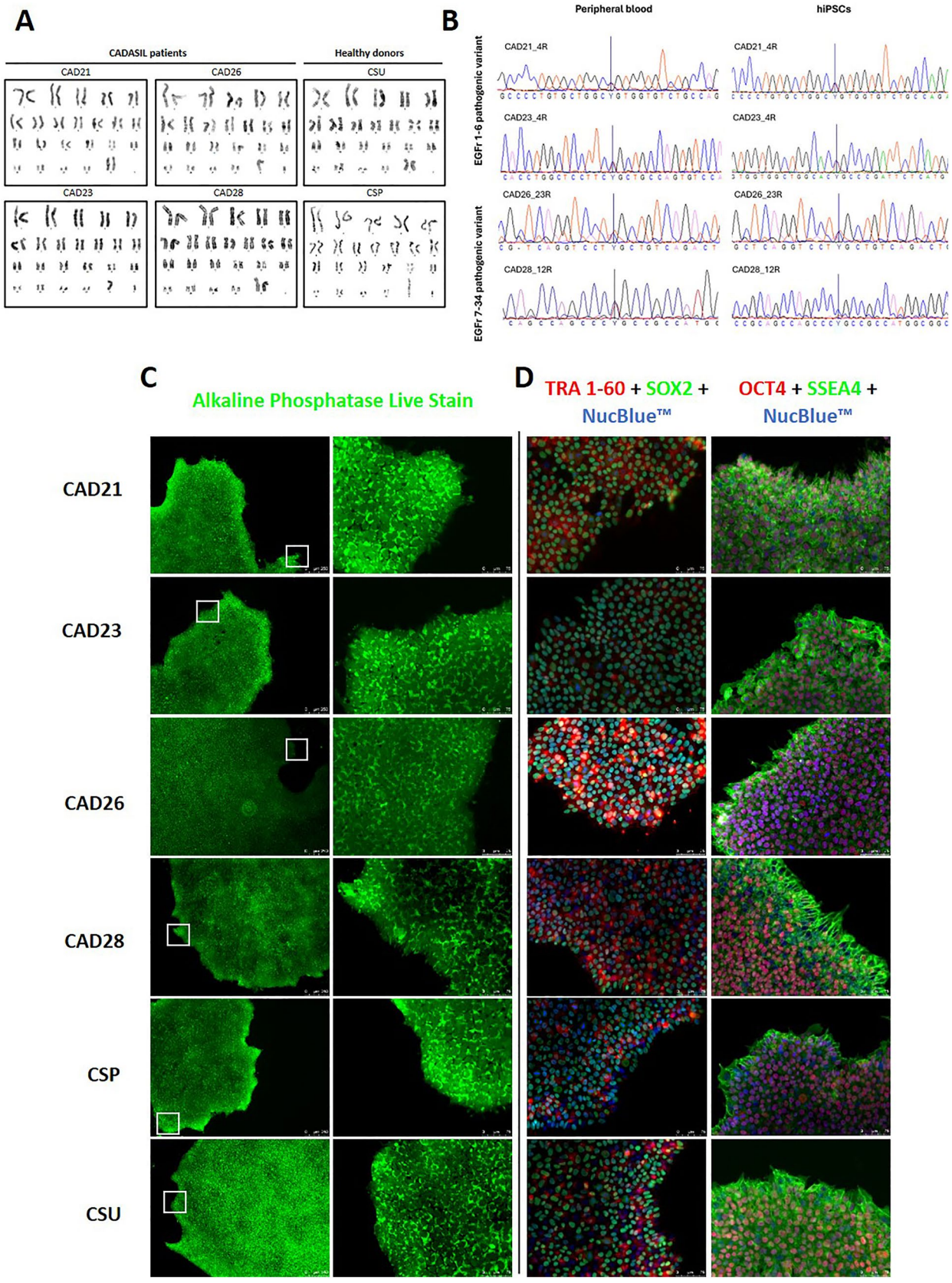
A
CADASIL patients
Healthy donors
CAD21
CAD26
CSU
CAD23
CAD28
CSP
B
Peripheral blood
hiPSCs
EGFr 1-6 pathogenic variant
EGFr 7-34 pathogenic variant
CAD21_4R
CAD23_4R
CAD26_23R
CAD28_12R
C
Alkaline Phosphatase Live Stain
D
TRA 1-60 + SOX2 + NucBlue™
OCT4 + SSEA4 + NucBlue™
CAD21
CAD23
CAD26
CAD28
CSP
CSU

◂**Fig. 2** Genetic and molecular characterization of the six human-induced pluripotent stem cells (hiPSCs) lines derived from the four CADASIL patients (coded as CAD21, CAD23, CAD26 and CAD28) and two control subjects (coded as CSU and CSP). **a** Karyotype analysis of the six generated hiPSCs lines from CADASIL patients and control subjects. **b** Analysis of *NOTCH3* mutations by Sanger sequencing in peripheral blood and the corresponding generated hiPSCs. Genetic variants of the *NOTCH3* gene are located in exon 3 in patient CAD23, exon 4 in patient CAD21, exon 11 in CAD28 and exon 23 in CAD26. **c** Analysis of alkaline phosphatase (AP) staining in the generated hiPSCs lines. Scale bar in the left panels: 250 µm (5×). Magnification (white square on the right panel) is shown in the left panels. Scale bar 75 µm (20×). **d** Expression analysis of pluripotency markers by immunocytochemical staining. Images are composed of NucBlueTM (blue) and specific markers: TRA 1–60 (red) in combination with SOX2 (green), SSEA4 (green) in combination with OCT4 (red). Scale bar for 4 pluripotent markers: 75 µm (20×)

CADASIL (Fig. 2a). Additionally, screening of *NOTCH3* mutations via Sanger sequencing was performed using PBMCs and the generated hiPSCs to confirm that the Sendai Virus (SeV) reprograming process did not affect the *NOTCH3* mutant sequence (Fig. 2b). Short tandem repeats (STRs) analysis verified the match between hiPSCs generated from the original PBMCs (Table 1S). Immunocytochemical analysis showed similar expression patterns of alkaline phosphatase (AP) and pluripotency markers (OCT4, SOX2, SSEA4, and TRA1-60) in the generated hiPSCs lines (Fig. 2c, d, respectively) and those from control subjects. Similar changes in the pluripotency markers were observed via flow cytometry (Fig. 1SA) and RT-qPCR (SOX2 and OCT4; Fig. 1SB and 1SC, respectively).

Final characterization was performed by testing the differentiation of the cell lines into the three embryonic germ layers: Ectoderm, endoderm, and mesoderm. Differentiation into the three germ layers was induced using a commercially available kit and examined via immunobiological analysis (Fig. 2SA) and RT-qPCR (SOX17, NCAM1, and PAX6; Fig. 2SB). The six generated cell lines successfully differentiated into the three germ layers, showing high expression levels of SOX17, NCAM1, and PAX6 markers. No differences were observed in donor *vs* patient cell lines and EGFr 1–6 *vs* 7–34 variants.

Examination of Notch3 Accumulation in hiPSCs

To determine whether the pathological Notch3 accumulation can be detected at the hiPSCs level, full-length Notch3 expression levels were first analyzed in the six generated cell lines by enzyme-linked immunosorbent assay (ELISA). We found higher Notch3 protein levels in the hiPSCs lines of patients with CADASIL than in those of the controls, with a significant difference in EGFr 1–6 variants ($p = 0.0051$; Fig. 3a). The differences were more pronounced when a more specific immunocytochemical analysis was used, where both receptor domains, NECD and NICD, were analyzed separately. We observed higher immunostaining accumulation of both NECD and NICD in the cell lines with EGFr 1–6 variants than in those with EGFr 7–34 variants and control cell lines. NECD was more aggregated around the plasma membrane (Fig. 3b), whereas NICD showed a diffused pattern throughout the cytoplasm (Fig. 3c). Quantitative analysis of the fluorescence intensity of NICD is shown in Fig. 3d and NECD is shown in Fig. 3e.

Qualitative Proteomic Analysis of hiPSCs Derived from Patients with CADASIL and Controls

To characterize the generated hiPSCs lines and evaluate whether the position of the pathogenic variant in *NOTCH3* affects its cell proteomic profile, we performed two different proteomic assays. First, descriptive data-dependent acquisition (DDA) analysis (qualitative analysis) was performed to compare patients *vs* controls and EGFr 1–6 *vs* 7–34 variants. Then, quantitative sequential window acquisition of all theoretical mass spectra (SWATH-MS) analysis was performed to determine the dysregulated protein levels in CADASIL cell lines.

DDA analysis (patients *vs* controls) revealed 298 proteins found only in the CADASIL samples (Venn diagram, Fig. 4a). The Search Tool for the Retrieval of Interacting Genes/Proteins (STRING) database (https://string-db.org/) and Gene Ontology pathway enrichment analyses revealed that the 298 proteins selectively detected in CADASIL samples were related to cytoskeletal reorganization processes, filament organization and supramolecular fiber organization (Fig. 4b).

Subsequent Functional Enrichment Analysis Tool software (FunRich) was used to analyze the potential biological processes related to CADASIL by comparing samples between EGFr 1–6 variant *vs* control and EGFr 7–34 variant *vs* control. The following biological functions were found in both CADASIL groups (compared to the control group): (i) a decrease in the inhibitory mechanisms of contraction and (ii) a lower positive regulation of contraction and processes associated with VSMCs. Processes related to (i) cytoskeletal reorganization, (ii) negative regulation of vasculogenesis, and (iii) autophagy were enhanced (Fig. 4c, d).

Comparative protein expression analyses of the two CADASIL groups were performed as a secondary analysis. As shown in the Venn diagram, 161 proteins were common for both EGFr 1–6 and 7–34 variants (Fig. 5a). STRING analysis revealed that these proteins played important roles in (i) central nervous system diseases, (ii) neurodegenerative diseases, (iii) amyloidosis, and (iv) vascular function impairment (Fig. 5b). Notably, 25 proteins were specifically detected with the EGFr 1–6 variants (Fig. 5c) and involved in (i) cellular structure and maintenance and (ii) cytoskeleton formation. In the EGFr 7–34 pathogenic variant group, 88

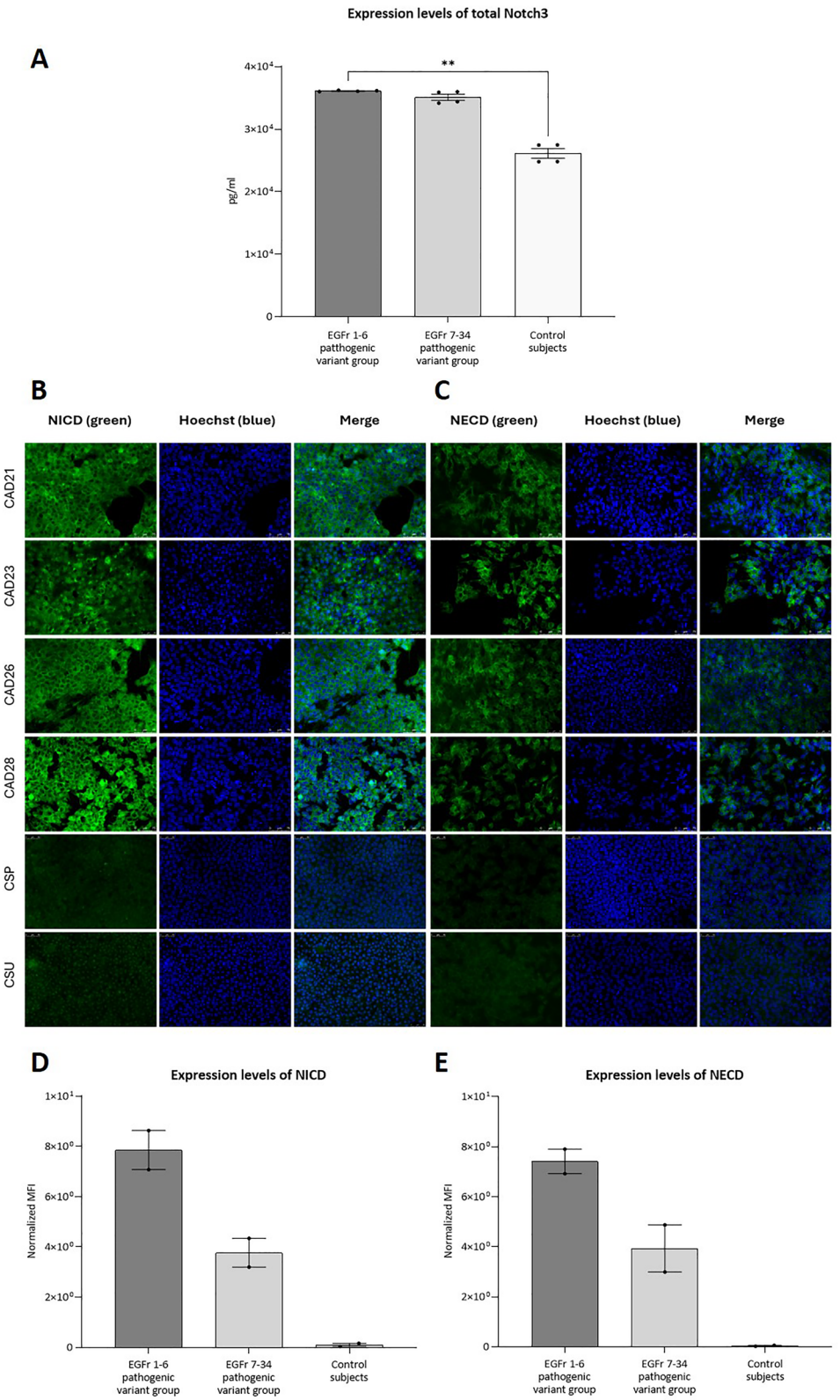

Fig. 3 Analysis of full-length Notch3 receptor and Notch intracellular domain (NICD) and Notch extracellular domain (NECD) in the six generated human induced pluripotent stem cell (hiPSC) lines from CADASIL patients and controls. **a** Comparative analysis of full-length Notch3 expression levels (pg/ml) in hiPSCs from patients with CADASIL EGFr 1–6 pathogenic group (patients coded as CAD21 and CAD23), 7–34 pathogenic group (patients coded as CAD26 and CAD28) and control subjects. $^{**}p < 0.01$ compared to control group; n = 4 per group (four replicates/hiPSCs lines), **b** Immunocytochemical staining analysis of NICD (green, lest panels), Hoechst (blue, middle panels) and merge images (right panels) and **c** immunocytochemical staining analysis of NECD (green, left panels), Hoechst (blue, middle panels) and merge images (right panels) of the six generated hiPSCs lines from the four CADASIL patients (coded as CAD21, CAD23, CAD26 and CAD28) and two control subjects (coded as CSU and CSP). Scale bar: 75 µm (20×). **d** Quantitative fluorescence analysis of NICD and (**E**) NECD immune staining in EGFr 1–6 and 7–34 pathogenic variants and controls. In both analyses, data are expressed as mean fluorescence of intensity (MFI) normalized to Hoechst expression. Data are expressed as normalized MFI, with each group containing n = 2 per group (two replicates/hiPSCs lines). Data are compared with the control group

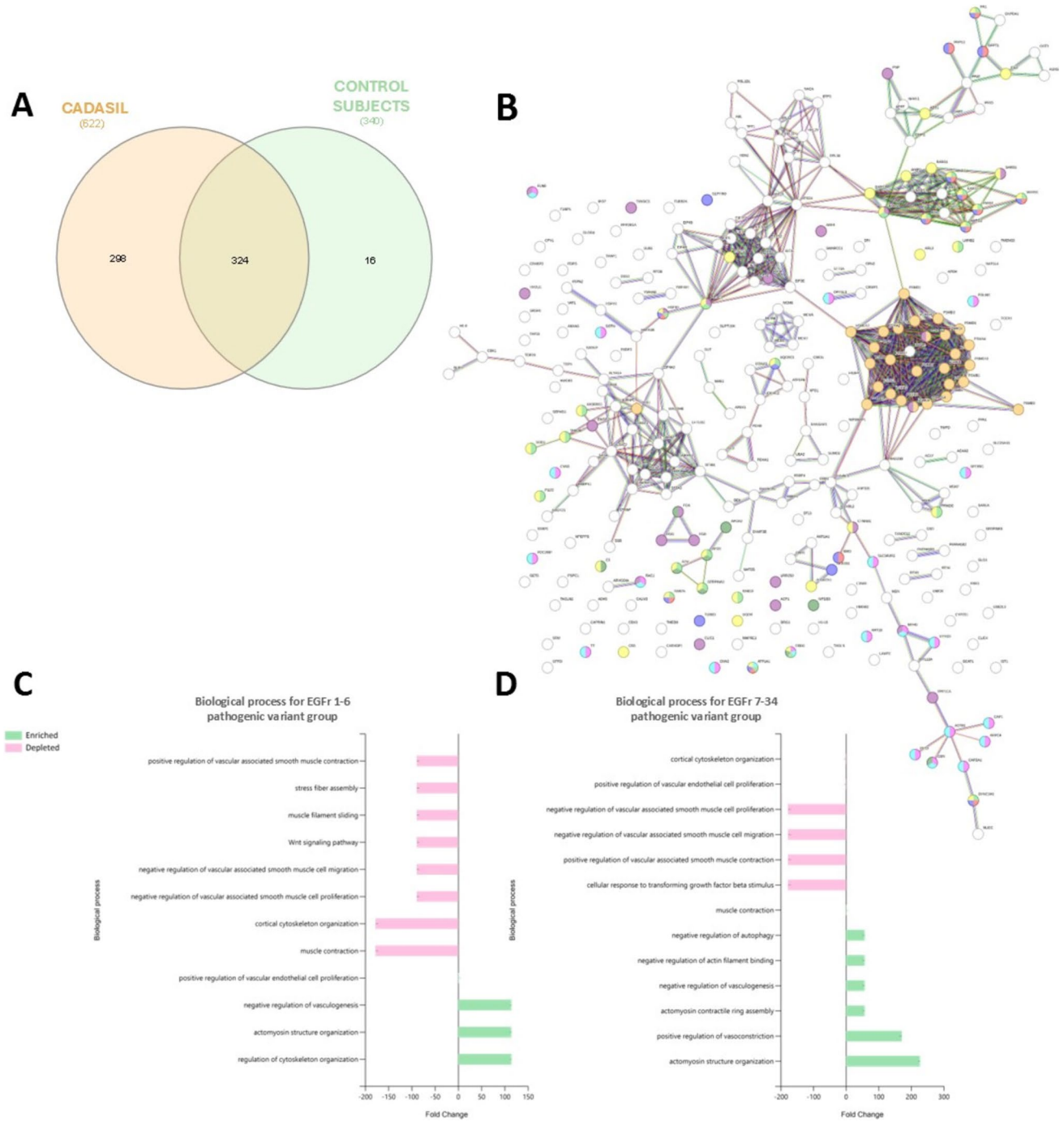

Fig. 4 Qualitative proteomic analysis of the six human induced pluripotent stem cell (hiPSCs) lines generated from CADASIL patients and controls. **a** Data-dependent acquisition (DDA) analysis comparing CADASIL patient *vs* controls are represented by a Venn diagram. **b** Search Tool for the Retrieval of Interacting Genes/Proteins (STRING) database (https://string-db.org/) and Gene Ontology pathway enrichment analyses. Enrichment analyses revealed that the 298 proteins selectively detected in CADASIL samples were associated with cytoskeletal organisation (light blue bubbles), filament organization (light green and dark green bubbles) and supramolecular fiber organization (yellow and orange bubbles). Other proteins were found to be involved in the VEGFA-VEGFR2 signaling pathway (red bubbles) and in amyloidosis processes (dark blue bubbles). **c** Functional Enrichment Analysis Tool (FunRich) software analysis of potential biological processes related to CADASIL by comparing samples between EGFr 1–6 variant *vs* control and **d** EGFr 7–34 variant *vs* control. Up-regulated pathways are labelled in green and down-regulated in red

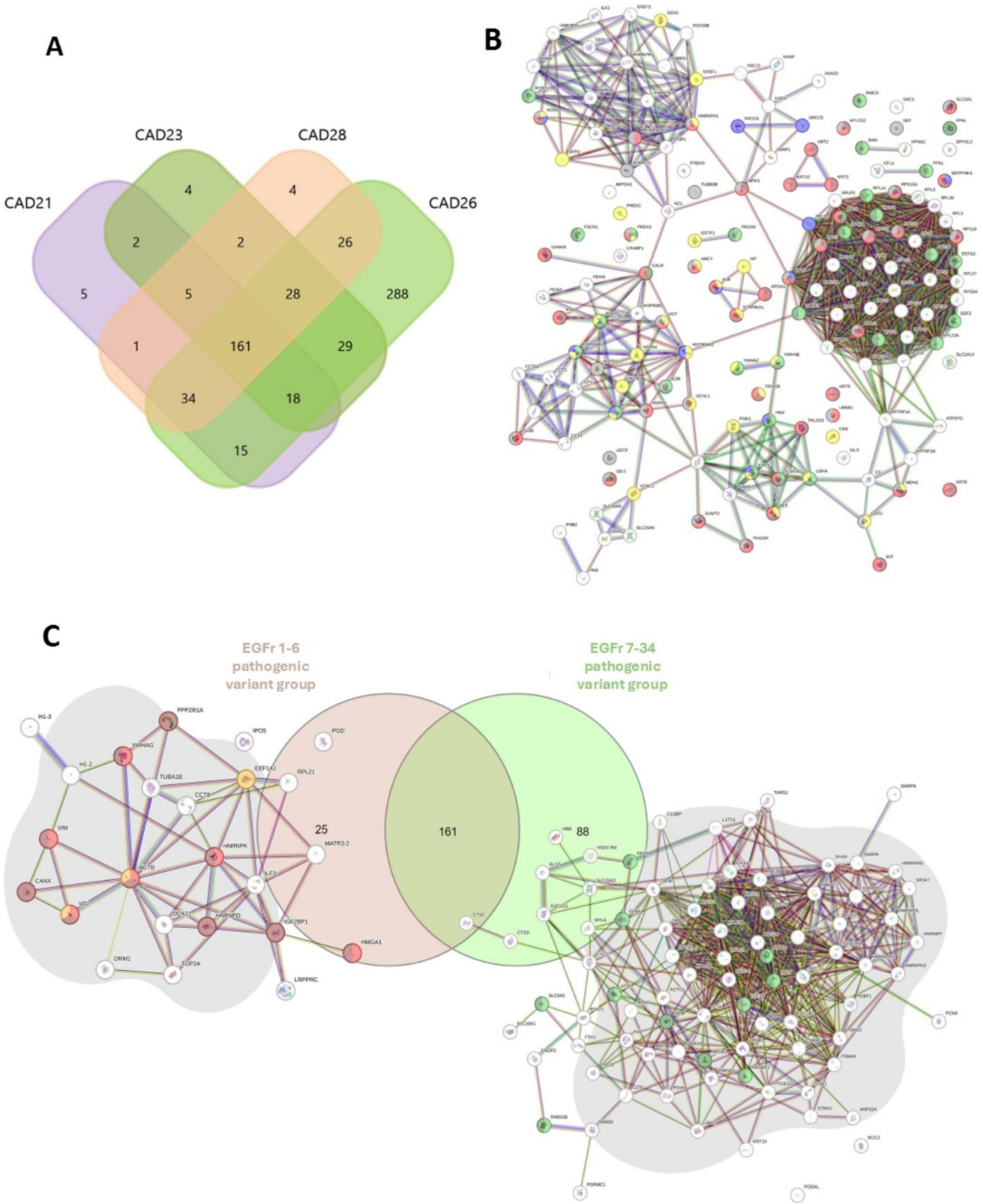
A
CAD23
CAD28
CAD21
CAD26
4
4
2
2
26
5
5
28
288
1
161
29
34
18
15
B
C
EGFr 1-6 pathogenic variant group
EGFr 7-34 pathogenic variant group
25
161
88
MATR3-2
HMGA1
IGF2BP1
LRPPRC
HNRNPK
ACTB
CANX
VIM
TUBA1B
EEF1A1
RPL21
PPP2R1A
YWHAG
IPO5
PGD
TOP2A
ORM1

◂**Fig. 5** Data-dependent acquisition (DDA) analysis of the generated human induced pluripotent stem cell (hiPSC) lines from CADASIL patients. **a** DDA analysis comparing the four CADASIL hiPSC lines (coded as CAD21, CAD23, CAD26 and CAD28) and represented by a Venn diagram. **b** Search Tool for the Retrieval of Interacting Genes/Proteins (STRING) database (https://string-db.org/) with a minimum interaction score threshold of 0.900 and Gene Ontology pathway enrichment analyses. The enrichment analyses revealed 161 common proteins in four CADASIL cell lines. These common proteins were involved in the formation of the vasculature (red and blue bubbles), maintenance of the cytoskeleton and cell structure (light green and dark green bubbles), pathways of altered brain morphology (gray bubbles) and other proteins described in the context of stroke (yellow bubbles). (**C**) DDA analysis comparing the CADASIL EGFr 1–6 pathogenic group (patients coded as CAD21 and CAD23) with the 7–34 pathogenic group (patients coded as CAD26 and CAD28), represented by a Venn diagram. Twenty-five proteins were detected exclusively in the EGFr 1–6 pathogenic variant group and 88 in the EGFr 7–34 pathogenic variant group

specific proteins were highly related to (i) cadherin binding, (ii) cytoskeleton stability, and (iii) cellular cohesion (Fig. 5d).

Quantitative Proteomic Analysis of hiPSCs Derived from Patients with CADASIL and Controls

Quantitative analysis of SWATH-MS data was performed. Similar to DDA analysis, in silico interactions of the dysregulated proteins were analyzed using the STRING software with Gene Ontology enrichment, metabolic functions, and pathways. Three different comparative analyses were performed: (i) EGFr 1–6 variants *vs* control, (ii) EGFr 7–34 variants *vs* control, and (iii) EGFr 1–6 *vs* EGFr 7–34 variants.

In the first group (EGFr 1–6 variants *vs* control), 64 proteins were dysregulated ($p < 0.05$; Fig. 6a; Table 2S) and involved in (i) cadherin binding, (ii) cell structure maintenance, and (iii) metabolic pathways related to neurodegenerative processes (Fig. 6b).

In the second group (EGFr 7–34 variants *vs* control), 85 proteins were dysregulated ($p < 0.05$; Fig. 6c; Table 3S) and involved in (i) cadherin binding and (ii) cell adhesion (Fig. 6d).

Finally, in the third group, when EGFr 1–6 *vs* EGFr 7–34 were compared, 49 proteins were found to be dysregulated ($p < 0.05$; Fig. 6e; Table 4S). These proteins are involved in processes related to (i) cellular organization, (ii) conservation and adhesion pathways, and (iii) formation of the extracellular matrix and cytoskeleton restructuring (Fig. 6f).

Among the proteins identified in SWATH-MS analysis, vimentin was found that showed significantly dysregulated, mainly in the EGFr 1–6 CADASIL group. Specifically, EGFr 1–6 *vs* 7–34 variant ($p = 0.0371$) and EGFr 1–6 variant *vs* control ($p = 0.0271$; Fig. 7a). The expression levels of vimentin were subsequently validated by ELISA, observing significant differences between the EGFr 1–6 variant *vs* control ($p = 0.0098$; Fig. 7b).

Next, comparative analysis of DDA and SWATH-MS data was performed (Venn diagram, Fig. 3S). Overlapping of 29 common CADASIL proteins was detected. STRING analysis of these 29 proteins using both qualitative and quantitative methods revealed similar biological pathways. These proteins were associated with cell adhesion molecules that enable cells to adhere to each other and the extracellular matrix, facilitating the formation and maintenance of tissue structures (Fig. 4S).

Discussion

Position of the *NOTCH3* cysteine-altering missense variant is an important indicator of disease severity (Cho et al., 2021, 2022; Gravesteijn et al., 2022; Mukai et al., 2020; Rutten et al., 2016, 2019). However, this clinical association has never been analyzed in an experimental setting. We previously reported that *NOTCH3* mutations do not limit the cell reprogramming, demonstrating the potential of hiPSCs technology to study and model CADASIL pathology (Fernandez-Susavila et al., 2018). Subsequently, several studies generated hiPSCs from CADASIL somatic cells as human CADASIL models, further increasing the knowledge on CADASIL pathology (Ahn et al., 2024; Chen et al., 2020; Fernandez-Susavila et al., 2018; Jalil et al., 2021; Kelleher et al., 2019; Ling et al., 2019; Manini & Pantoni, 2021; Wang et al., 2024; Yamamoto et al., 2020; Zhang et al., 2023). In this new study, we evaluated how the position of the mutant variant affects the level of disease severity using hiPSCs cell technology.

Using the non-integrative SeV reprogramming kit, we demonstrated that the efficiency of reprogramming from PBMCs was similar in all tested cases of CADASIL, regardless of the mutation position, with similar success observed in the hiPSCs generated from healthy donors. These results suggest that the position of the *NOTCH3* mutation does not affect cell reprogramming to generate hiPSCs.

Once the hiPSCs from patients and controls were generated and characterized, we wanted to see whether the position of the *NOTCH3* variant had any effect on the cells. With this purpose, first, we analyzed the Notch3 protein accumulation and secondly, we developed a comparative proteomic analysis.

The key vascular pathological features of CADASIL are the aggregation and staining of NECD in the vessel wall and presence of GOM deposits (Joutel et al., 2000; Opherk et al., 2009). Moreover, patients with CADASIL with EGFr 7–34 variants exhibit significantly lower vascular Notch3 aggregation than those with EGFr 1–6 variants, indicating variant position as a factor affecting the disease severity (Gravesteijn et al., 2022). Consistently with the pathogenesis of the disease, we observed an association between Notch3 accumulation and *NOTCH3* variant position in CADASIL.

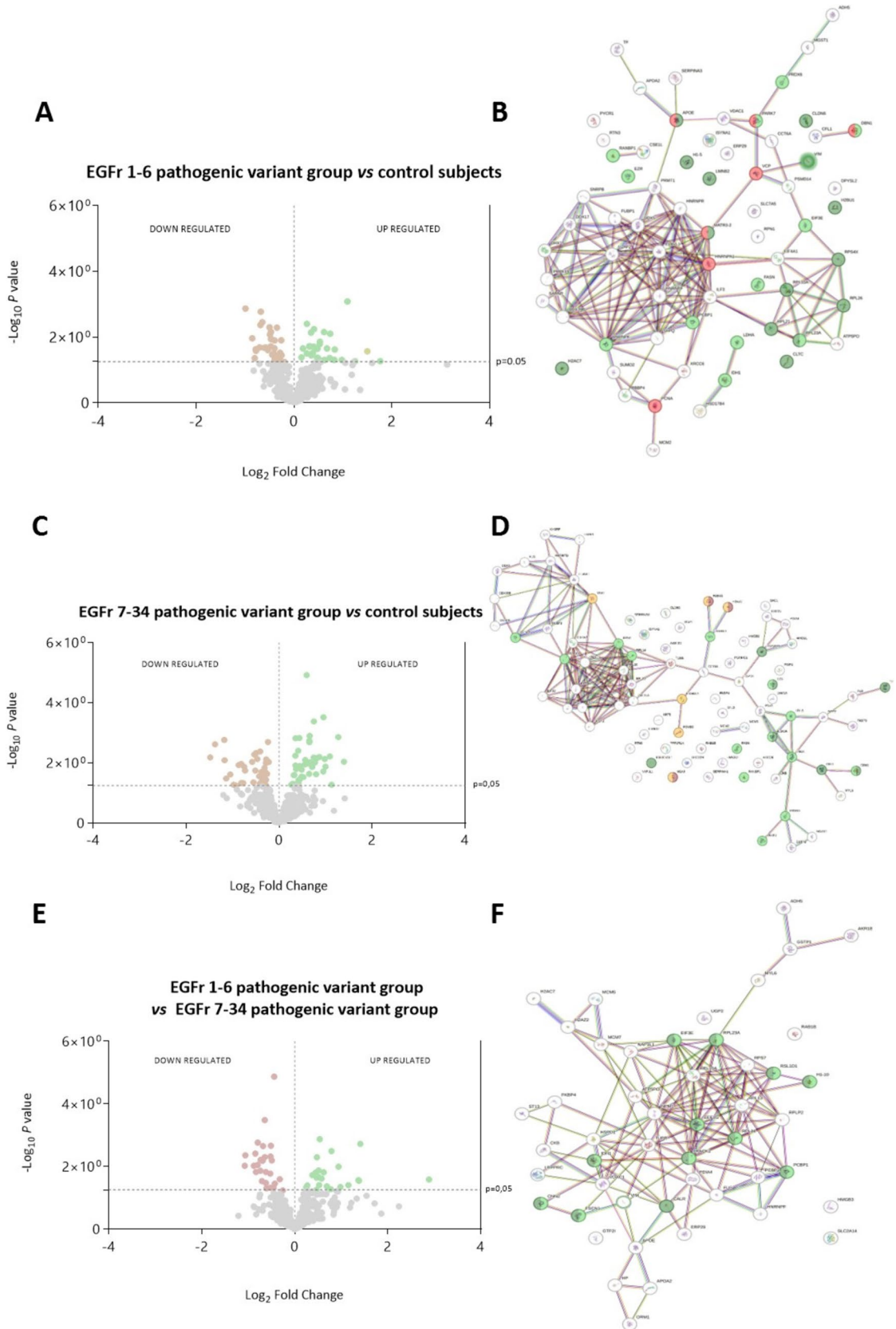
A
EGFr 1-6 pathogenic variant group vs control subjects
DOWN REGULATED
UP REGULATED
p=0.05
-Log10 P value
Log2 Fold Change
B
C
EGFr 7-34 pathogenic variant group vs control subjects
DOWN REGULATED
UP REGULATED
p=0,05
-Log10 P value
Log2 Fold Change
D
E
EGFr 1-6 pathogenic variant group
vs EGFr 7-34 pathogenic variant group
DOWN REGULATED
UP REGULATED
p=0,05
-Log10 P value
Log2 Fold Change
F

◂**Fig. 6** Quantitative sequential window acquisition of all theoretical mass spectra (SWATH-MS) analysis comparing EGFr 1–6 variants *vs* control, EGFr 7–34 variants *vs* control and EGFr 1–6 *vs* EGFr 7–34 variants. **a** Volcano plots comparing EGFr 1–6 variants *vs* control samples. **b** Enrichment analyses of the EGFr 1–6 pathogenic variant group *vs* controls detected dysregulated proteins related to cadherin binding pathways (light green bubbles) and cell structure (dark green bubbles), and are also described in neurodegeneration processes (red bubbles). **c** Volcano plots comparing EGFr 7–34 variants with control samples. **d** Dysregulated proteins in the EGFr 7–34 pathogenic variant group *vs* controls. These proteins are involved in the organization of actin filaments (dark green bubbles) and cadherin binding proteins (light green bubbles) appear. In addition, proteins related to the Notch signaling pathway (orange bubbles) and Notch transcription and translation processing (maroon bubbles) were present. **e** Volcano plots comparing EGFr 1–6 *vs* 7–34 variants. **f** Enrichment analyses comparing EGFr 1–6 *vs* 7–34 variants detected dysregulated proteins related to cadherin binding (light green bubbles) and cell binding processes (dark green bubbles). In the volcano plots, red dots represent $p < 0.05$ and fold index < 1 and green dots represent data with $p < 0.05$ and fold rate > 1 in comparisons between the different experimental groups

Specific immunostaining analysis also revealed similar patterns at the pluripotent stem cell level for both receptor domains; NICD and NECD. Many studies have reported the progressive accumulation of NECD as a major driver of arterial VSMC loss in CADASIL (Dupre et al., 2024; Joutel et al., 2000; Monet-Lepretre et al., 2013), meanwhile NICD accumulation has been poorly explored (Joutel et al., 2000). Our immunoassay analysis revealed an association between cytoplasmic signals of NICD and CADASIL severity. However, this interpretation should be treated with caution, as the commercial antibodies for Notch3 receptor are mainly designed against NECD (Ghezali et al., 2018), while specificity for NICD is not fully guaranteed.

On the other hand, and consistent with previous reports in "omic" analysis in CADASIL (Muino et al., 2021a), quantitative and qualitative proteomic analyses revealed proteomic changes associated with the *NOTCH3* variant position. Specifically, we observed protein changes related with cytoskeletal reorganization mechanisms, and a correlation between vimentin expression and CADASIL EGFr 1–6 pathogenic variants. Vimentin is a type III intermediate filament protein that anchors and supports organelles within the cytosol (Engeland et al., 2019; Vermeire et al., 2023) and regulates the structural homeostasis of the arterial wall. The critical role of vimentin in CADASIL has been also reported in previous studies using VSMCs differentiated from hiPSCs of patients with CADASIL (Ling et al., 2019). These findings suggest that cytoskeleton-related proteins, such as vimentin, may have a valuable role as clinical biomarkers for CADASIL prognosis.

To the best of our knowledge, this study represents the first experimental approach to evaluate the clinical associations between *NOTCH3* pathogenic genetic variants and CADASIL severity. However, this study has some limitations that should be addressed in future studies. Control subjects were not age-matched to the patients with CADASIL, and isogenic human iPSCs, which are more appropriate as controls, were not used in this study. Although CADASIL is a rare pathology, a larger sample size should be assessed in future studies to validate our findings. Furthermore, future studies should examine the differentiation of hiPSCs into pathogenic cell types (VSMCs) to determine the impact of *NOTCH3* mutation position on cell dysfunction.

In conclusion, this study revealed that EGFr 1–6 pathogenic genetic variant was associated with altered cytoskeletal reorganization mechanisms and elevated Notch3 expression levels, at least at the pluripotent stem cell level. These findings are aligned with the clinical association between the pathogenic *NOTCH3* variants and CADASIL severity. However, further analysis of VSMCs derived from hiPSCs is necessary to determine whether the vascular pathological accumulation of Notch3 differs between the different pathogenic genetic variants.

Materials and Methods

Patient Sample Collection and Ethical Issues

Four patients with CADASIL were prospectively recruited from the Hospital Univeristario Vall d´Hebron and Hospital Clínico Universitario of Santiago de Compostela. Three patients from Hospital Universitario Vall d´Hebron were selected based on the "CADAGENIA" registry (Muino et al., 2021b), which is a prospective registry containing the clinical and epidemiological, neuroimaging, and genetic data of patients with genetic variants in *NOTCH3*. This study was approved by the Ethics Committee of Hospital de la Santa Creu i Sant Pau (IIBSP-CAD-2019-56). The fourth patient with CADASIL and two control volunteers were recruited from the Stroke Unit of the Hospital of Santiago de Compostela with approval from the Scientific Ethics Committee for the Region of Santiago-Lugo (protocol number: 2016/450). All participants received detailed information prior to blood and clinical data collection.

Patient Sample Collection and Peripheral Blood Mononuclear Cells (PBMCs) Isolation

hiPSCs were generated from PBMCs of the patients and control volunteers. Briefly, 8 mL of blood was collected in BD Vacutainer BD K2 EDTA tubes (ref. BDN-368171; Becton, Dickinson and Company, Franklin Lakes, NJ, USA) via direct puncture of a vein in the antecubital area of the arm. PBMCs were isolated from the whole blood samples of all participants. Then, 8 mL of collected blood was combined with 8 mL of 2% phosphate-buffered saline + fetal bovine

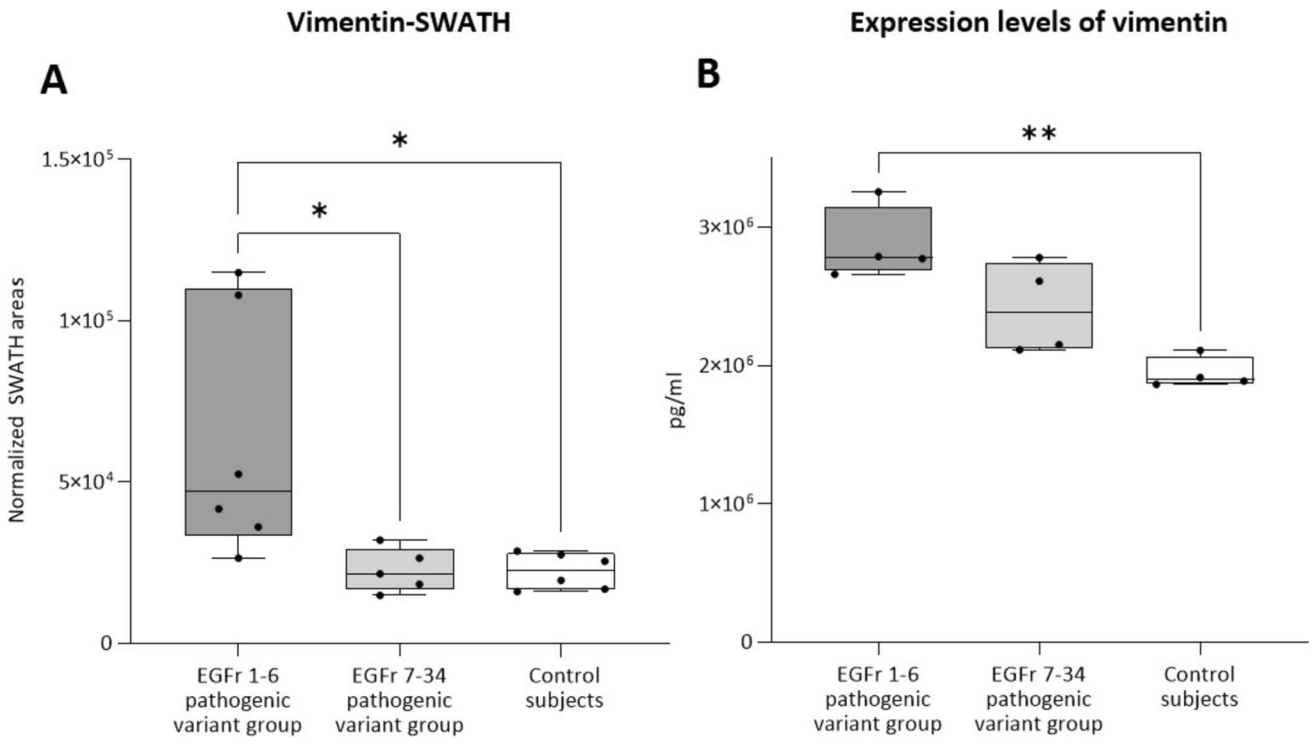

Fig. 7 Validation of vimentin data. **a** Quantitative sequential window acquisition of all theoretical mass spectra (SWATH-MS) analysis of vimentin in patients with CADASIL EGFr 1–6 pathogenic group (patients coded as CAD21 and CAD23), 7–34 pathogenic group (patients coded as CAD26 and CAD28) and control subjects (coded as CSU and CSP). **b** Comparative analysis if vimentin levels (pg/ml) in human induced pluripotent stem cell (hiPSC) lines from patients with CADASIL EGFr 1–6 pathogenic group (patients coded as CAD21 and CAD23), 7–34 pathogenic group (patients coded as CAD26 and CAD28) and control subjects (coded as CSU and CSP). *$p < 0.05$ and **$p < 0.01$ compared to control group; $n = 6$ per group (sex replicates/hiPSCs lines)

serum (Cat. No. A5670501; Thermo Fisher, Cham, Switzerland) and diluted with 15 mL of Lymphoprep (Cat. No. 07801; STEMCELL Technologies, Vancouver, BC, Canada) in SepMate-50 tubes designed for PBMCs isolation (Sarkar et al., 2024).

PBMCs Reprogramming

Following our previously established method for human cell programming in patients with CADASIL (Fernandez-Susavila et al., 2018), 5×10^5 PBMCs were seeded per well in 12-well Corning plates (Cat. No. 3513; Corning, Inc., Corning, NY, USA) and cultured using the StemPro-34 SFM 1X media kit (Cat. No. 10639011; Thermo Fisher Scientific, Carlsbad, CA, USA). To stimulate hematopoietic cell proliferation, the medium was supplemented with the StemSpan CC100 cytokine cocktail (Cat. No. 02690; STEMCELL Technologies). After four days, half of the culture medium was refreshed. On the fifth day, the cells were transduced using the Cytotune 2.0 reprogramming kit (Thermo Fisher Scientific, Waltham, MA, USA; cat. no. A16517), with the non-integrating Sendai virus (SeV) (Sarkar et al., 2024) to introduce the reprogramming factors (Klf4–Oct3/4–Sox2, cMyc, and Klf4). After 24 h of viral transduction, the cells were harvested, and the virus was removed via centrifugation at 200×*g* for 5 min at room temperature. The cultured cells were maintained for 3–4 weeks on the Corning Matrigel hESC-qualified matrix (Cat. No. 354277; Corning, Inc.) in Costar 6-well plates (Cat. No. 3516; Corning, Inc.) using the mTeSR Plus media kit (Cat. No. 1000276; STEMCELL Technologies; schematic of the reprogramming process is shown in Fig. 5S).

hiPSCs Characterization

The following standardized tests were used to characterize the cell lines derived from the patients with CADASIL and healthy donors: Moore et al., (2023) (1) karyotype analysis, (2) Sanger sequencing of *NOTCH3* mutant gene after cell reprogramming, (3) STR analysis, (4) AP activity analysis, (5) analysis of pluripotency markers, and (6) analysis of the hiPSCs ability to differentiate into the three embryonic germ layers. Technical details of hiPSCs characterization are provided in the Supplemental Information and Tables 5S–11S.

Notch3 Protein and Proteomic Analyses

After hiPSCs characterization, the six generated cell lines were analyzed by comparing their Notch3 protein accumulation and proteomic profiles (described in detail in the Supplementary Information).

Data Processing and Statistical Analyses

All results were statistically analyzed using the GraphPad Prism v.9.0.2 software (GraphPad Software, La Jolla, CA, USA). In all graphs, bars indicate the mean ± standard error of the mean. Statistical analysis results of each test are explained in detail in the Supplementary Information.

Supplementary Information The online version contains supplementary material available at https://doi.org/10.1007/s12017-025-08840-6.

Author Contributions All authors contributed to the study conception and design. Material preparation, data collection and analysis were performed by Ana Bugallo-Casal, Elena Muiño, Susana B. Bravo, Pablo Hervella, Susana Arias-Rivas, Manuel Rodríguez-Yañez, Enrique Vara-León, Rita Quintas-Rey, Lara Pérez-Gayol, Olga Maisterra-Santos, Jesús Pizarro-Gonzálvez, María Rosa Martorell-Riera and Cristòfol Vives-Bauzá. The first draft of the manuscript was written by Elena Muiño, Israel Fernández-Cadenas, José Castillo, and Francisco Campos and all authors commented on previous versions of the manuscript. All authors read and approved the final manuscript.

Funding This study has been funded by Instituto de Salud Carlos III (ISCIII) through the project PI17/00540, PI20/01014, PI23/000890, RICORS-ICITUS RD21/0006/0003, RD21/0006/0004, RD24/0009/0022, RD24/0009/0017 and AC23-2/00029. AC23-2/00029 (named as CADANHIS) project has been supported by the EJP RD—European Joint Programme on Rare Diseases—Joint Transnational Call 2023 for Rare Diseases Research Project (JTC 2023). The EJP RD initiative has received funding from the European Union's Horizon 2020 research and innovation programme under grant agreement N°825575. Finally, this work was supported by grants from the Instituto de Salud Carlos III, PReDICT Project (PMPER24/00021) together with Next-Generation EU funds that finance the actions of the Recovery and Resilience Mechanism.

Data Availability Data are available upon reasonable request from the corresponding author.

Declarations

Conflict of interest The authors have no relevant financial or non-financial interests to disclose.

Ethical Approval This study was performed in line with the principles of the Declaration of Helsinki. Approval was granted by the Ethics Committee of Hospital de la Santa Creu i Sant Pau (IIBSP-CAD-2019-56) and Ethics Committee for the Region of Santiago-Lugo (protocol number: 2016/450. Informed consent was obtained from all individual participants included in the study.

References

Ahn, Y., An, J. H., Yang, H. J., Lee, W. J., Lee, S. H., Park, Y. H., Lee, J. H., Lee, H. J., Lee, S. H., & Kim, S. U. (2024). Blood vessel organoids generated by base editing and harboring single nucleotide variation in Notch3 effectively recapitulate CADASIL-related pathogenesis. *Molecular Neurobiology*. https://doi.org/10.1007/s12035-024-04141-4

Brulin, P., Godfraind, C., Leteurtre, E., & Ruchoux, M. M. (2002). Morphometric analysis of ultrastructural vascular changes in CADASIL: Analysis of 50 skin biopsy specimens and pathogenic implications. *Acta Neuropathologica, 104*(3), 241–248. https://doi.org/10.1007/s00401-002-0530-z

Chabriat, H., Joutel, A., Dichgans, M., Tournier-Lasserve, E., & Bousser, M. G. (2009). Cadasil. *Lancet Neurology, 8*(7), 643–653. https://doi.org/10.1016/S1474-4422(09)70127-9

Chabriat, H., Vahedi, K., Bousser, M. G., Iba-Zizen, M. T., Joutel, A., Nibbio, A., Nagy, T. G., Tournier Lasserve, E., Krebs, M. O., Julien, J., Ducrocq, X., Levasseur, M., Mas, J. L., Dubois, B., Homeyer, P., & Lyon-Caen, O. (1995). Clinical spectrum of CADASIL: a study of 7 families. *Lancet, 346*(8980), 934–939. https://doi.org/10.1016/s0140-6736(95)91557-5

Chen, G., Li, Z., Liu, Y., Chen, D., Beers, J., Cudrici, C., Ferrante, E. A., Schwartzbeck, R., Dmitrieva, N., Yang, D., Zou, J., Iruela-Arispe, M. L., & Boehm, M. (2020). Generation of human induced pluripotent stem cells (NIHTVBi004-A, NIHTVBi005-A, NIHTVBi006-A, NIHTVBi007-A, NIHTVBi008-A) from 5 CADASIL patients with NOTCH3 mutation. *Stem Cell Research, 45*, 101821. https://doi.org/10.1016/j.scr.2020.101821

Cho, B. P. H., Jolly, A. A., Nannoni, S., Tozer, D., Bell, S., & Markus, H. S. (2022). Association of NOTCH3 variant position with stroke onset and other clinical features among patients with CADASIL. *Neurology, 99*(5), e430–e439. https://doi.org/10.1212/WNL.0000000000200744

Cho, B. P. H., Nannoni, S., Harshfield, E. L., Tozer, D., Graf, S., Bell, S., & Markus, H. S. (2021). NOTCH3 variants are more common than expected in the general population and associated with stroke and vascular dementia: An analysis of 200 000 participants. *Journal of Neurology, Neurosurgery and Psychiatry, 92*(7), 694–701. https://doi.org/10.1136/jnnp-2020-325838

Dupre, N., Gueniot, F., Domenga-Denier, V., Dubosclard, V., Nilles, C., Hill-Eubanks, D., Morgenthaler-Roth, C., Nelson, M. T., Keime, C., Danglot, L., & Joutel, A. (2024). Protein aggregates containing wild-type and mutant NOTCH3 are major drivers of arterial pathology in CADASIL. *Journal of Clinical Investigation*. https://doi.org/10.1172/JCI175789

Fernandez-Susavila, H., Mora, C., Aramburu-Nunez, M., Quintas-Rey, R., Arias, S., Collado, M., Lopez-Arias, E., Sobrino, T., Castillo, J., Dell'Era, P., & Campos, F. (2018). Generation and characterization of the human iPSC line IDISi001-A isolated from blood

cells of a CADASIL patient carrying a NOTCH3 mutation. *Stem Cell Research, 28*, 16–20. https://doi.org/10.1016/j.scr.2018.01.023

Ghezali, L., Capone, C., Baron-Menguy, C., Ratelade, J., Christensen, S., Ostergaard Pedersen, L., Domenga-Denier, V., Pedersen, J. T., & Joutel, A. (2018). Notch3(ECD) immunotherapy improves cerebrovascular responses in CADASIL mice. *Annals of Neurology, 84*(2), 246–259. https://doi.org/10.1002/ana.25284

Gravesteijn, G., Hack, R. J., Mulder, A. A., Cerfontaine, M. N., van Doorn, R., Hegeman, I. M., Jost, C. R., Rutten, J. W., & Lesnik Oberstein, S. A. J. (2022). NOTCH3 variant position is associated with NOTCH3 aggregation load in CADASIL vasculature. *Neuropathology and Applied Neurobiology, 48*(1), e12751. https://doi.org/10.1111/nan.12751

Gravesteijn, G., Munting, L. P., Overzier, M., Mulder, A. A., Hegeman, I., Derieppe, M., Koster, A. J., van Duinen, S. G., Meijer, O. C., Aartsma-Rus, A., van der Weerd, L., Jost, C. R., van den Maagdenberg, A., Rutten, J. W., & Lesnik Oberstein, S. A. J. (2020). Progression and classification of granular osmiophilic material (GOM) deposits in functionally characterized human NOTCH3 transgenic mice. *Translational Stroke Research, 11*(3), 517–527. https://doi.org/10.1007/s12975-019-00742-7

Gunda, B., Herve, D., Godin, O., Bruno, M., Reyes, S., Alili, N., Opherk, C., Jouvent, E., During, M., Bousser, M. G., Dichgans, M., & Chabriat, H. (2012). Effects of gender on the phenotype of CADASIL. *Stroke, 43*(1), 137–141. https://doi.org/10.1161/STROKEAHA.111.631028

Hack, R. J., Cerfontaine, M. N., Gravesteijn, G., Tap, S., Hafkemeijer, A., van der Grond, J., Witjes-Ane, M. N., Baas, F., Rutten, J. W., & Lesnik Oberstein, S. A. J. (2022). Effect of NOTCH3 EGFr group, sex, and cardiovascular risk factors on CADASIL clinical and neuroimaging outcomes. *Stroke, 53*(10), 3133–3144. https://doi.org/10.1161/STROKEAHA.122.039325

Hack, R. J., Gravesteijn, G., Cerfontaine, M. N., Santcroos, M. A., Gatti, L., Kopczak, A., Bersano, A., Duering, M., Rutten, J. W., & Lesnik Oberstein, S. A. J. (2023). Three-tiered EGFr domain risk stratification for individualized NOTCH3-small vessel disease prediction. *Brain, 146*(7), 2913–2927. https://doi.org/10.1093/brain/awac486

Hack, R. J., Rutten, J. W., Person, T. N., Li, J., Khan, A., Griessenauer, C. J., Regeneron Genetics, C., Abedi, V., Lesnik Oberstein, S. A. J., & Zand, R. (2020). Cysteine-altering NOTCH3 variants are a risk factor for stroke in the elderly population. *Stroke, 51*(12), 3562–3569. https://doi.org/10.1161/STROKEAHA.120.030343

Jalil, S., Keskinen, T., Maldonado, R., Sokka, J., Trokovic, R., Otonkoski, T., & Wartiovaara, K. (2021). Simultaneous high-efficiency base editing and reprogramming of patient fibroblasts. *Stem Cell Reports, 16*(12), 3064–3075. https://doi.org/10.1016/j.stemcr.2021.10.017

Joutel, A., Andreux, F., Gaulis, S., Domenga, V., Cecillon, M., Battail, N., Piga, N., Chapon, F., Godfrain, C., & Tournier-Lasserve, E. (2000). The ectodomain of the Notch3 receptor accumulates within the cerebrovasculature of CADASIL patients. *The Journal of Clinical Investigation, 105*(5), 597–605. https://doi.org/10.1172/JCI8047

Joutel, A., Corpechot, C., Ducros, A., Vahedi, K., Chabriat, H., Mouton, P., Alamowitch, S., Domenga, V., Cecillion, M., Marechal, E., Maciazek, J., Vayssiere, C., Cruaud, C., Cabanis, E. A., Ruchoux, M. M., Weissenbach, J., Bach, J. F., Bousser, M. G., & Tournier-Lasserve, E. (1996). Notch3 mutations in CADASIL, a hereditary adult-onset condition causing stroke and dementia. *Nature, 383*(6602), 707–710. https://doi.org/10.1038/383707a0

Joutel, A., Vahedi, K., Corpechot, C., Troesch, A., Chabriat, H., Vayssiere, C., Cruaud, C., Maciazek, J., Weissenbach, J., Bousser, M. G., Bach, J. F., & Tournier-Lasserve, E. (1997). Strong clustering and stereotyped nature of Notch3 mutations in CADASIL patients. *Lancet, 350*(9090), 1511–1515. https://doi.org/10.1016/S0140-6736(97)08083-5

Kelleher, J., Dickinson, A., Cain, S., Hu, Y., Bates, N., Harvey, A., Ren, J., Zhang, W., Moreton, F. C., Muir, K. W., Ward, C., Touyz, R. M., Sharma, P., Xu, Q., Kimber, S. J., & Wang, T. (2019). Patient-specific iPSC model of a genetic vascular dementia syndrome reveals failure of mural cells to stabilize capillary structures. *Stem Cell Reports, 13*(5), 817–831. https://doi.org/10.1016/j.stemcr.2019.10.004

Ling, C., Liu, Z., Song, M., Zhang, W., Wang, S., Liu, X., Ma, S., Sun, S., Fu, L., Chu, Q., Belmonte, J. C. I., Wang, Z., Qu, J., Yuan, Y., & Liu, G. H. (2019). Modeling CADASIL vascular pathologies with patient-derived induced pluripotent stem cells. *Protein & Cell, 10*(4), 249–271. https://doi.org/10.1007/s13238-019-0608-1

MacArthur, C. C., Pradhan, S., Wetton, N., Zarrabi, A., Dargitz, C., Sridharan, M., Jackson, S., Pickle, L., & Lakshmipathy, U. (2019). Generation and comprehensive characterization of induced pluripotent stem cells for translational research. *Regenerative Medicine, 14*(6), 505–524. https://doi.org/10.2217/rme-2018-0148

Manini, A., & Pantoni, L. (2021). CADASIL from bench to bedside: Disease models and novel therapeutic approaches. *Molecular Neurobiology, 58*(6), 2558–2573. https://doi.org/10.1007/s12035-021-02282-4

Monet-Lepretre, M., Haddad, I., Baron-Menguy, C., Fouillot-Panchal, M., Riani, M., Domenga-Denier, V., Dussaule, C., Cognat, E., Vinh, J., & Joutel, A. (2013). Abnormal recruitment of extracellular matrix proteins by excess Notch3 ECD: A new pathomechanism in CADASIL. *Brain, 136*(Pt 6), 1830–1845. https://doi.org/10.1093/brain/awt092

Moore, S., McGowan-Jordan, J., Smith, A. C., Rack, K., Koehler, U., Stevens-Kroef, M., Barseghyan, H., Kanagal-Shamanna, R., Hastings, R., & Committee, I. S. (2023). Genome mapping nomenclature. *Cytogenetic and Genome Research, 163*(5–6), 236–246. https://doi.org/10.1159/000535684

Muino, E., Fernandez-Cadenas, I., & Arboix, A. (2021a). Contribution of "Omic" studies to the understanding of CADASIL. A systematic review. *International Journal of Molecular Sciences*. https://doi.org/10.3390/ijms22147357

Muino, E., Maisterra, O., Jimenez-Balado, J., Cullell, N., Carrera, C., Torres-Aguila, N. P., Carcel-Marquez, J., Gallego-Fabrega, C., Lledos, M., Gonzalez-Sanchez, J., Olmos-Alpiste, F., Espejo, E., March, A., Pujol, R., Rodriguez-Campello, A., Romeral, G., Krupinski, J., Marti-Fabregas, J., Montaner, J., … Fernandez-Cadenas, I. (2021b). Genome-wide transcriptome study in skin biopsies reveals an association of E2F4 with cadasil and cognitive impairment. *Science and Reports, 11*(1), 6846. https://doi.org/10.1038/s41598-021-86349-1

Mukai, M., Mizuta, I., Watanabe-Hosomi, A., Koizumi, T., Matsuura, J., Hamano, A., Tomimoto, H., & Mizuno, T. (2020). Genotype-phenotype correlations and effect of mutation location in Japanese CADASIL patients. *Journal of Human Genetics, 65*(8), 637–646. https://doi.org/10.1038/s10038-020-0751-9

Opherk, C., Duering, M., Peters, N., Karpinska, A., Rosner, S., Schneider, E., Bader, B., Giese, A., & Dichgans, M. (2009). CADASIL mutations enhance spontaneous multimerization of NOTCH3. *Human Molecular Genetics, 18*(15), 2761–2767. https://doi.org/10.1093/hmg/ddp211

Rutten, J. W., Dauwerse, H. G., Gravesteijn, G., van Belzen, M. J., van der Grond, J., Polke, J. M., Bernal-Quiros, M., & Lesnik Oberstein, S. A. (2016). Archetypal NOTCH3 mutations frequent in public exome: Implications for CADASIL. *Annals of Clinical Translational Neurology, 3*(11), 844–853. https://doi.org/10.1002/acn3.344

Rutten, J. W., Van Eijsden, B. J., Duering, M., Jouvent, E., Opherk, C., Pantoni, L., Federico, A., Dichgans, M., Markus, H. S., Chabriat, H., & Lesnik Oberstein, S. A. J. (2019). The effect of

NOTCH3 pathogenic variant position on CADASIL disease severity: NOTCH3 EGFr 1–6 pathogenic variant are associated with a more severe phenotype and lower survival compared with EGFr 7–34 pathogenic variant. *Genetics in Medicine, 21*(3), 676–682. https://doi.org/10.1038/s41436-018-0088-3

Sarkar, J., Dhepe, S., Shivalkar, A., Kuhikar, R., More, S., Konala, V. B. R., Bhanushali, P., & Khanna, A. (2024). Generation of human-induced pluripotent stem cell line from PBMC of healthy donor using integration-free Sendai virus technology. *Stem Cell Research, 77*, 103402. https://doi.org/10.1016/j.scr.2024.103402

Singhal, S., Bevan, S., Barrick, T., Rich, P., & Markus, H. S. (2004). The influence of genetic and cardiovascular risk factors on the CADASIL phenotype. *Brain, 127*(Pt 9), 2031–2038. https://doi.org/10.1093/brain/awh223

Tikka, S., Mykkanen, K., Ruchoux, M. M., Bergholm, R., Junna, M., Poyhonen, M., Yki-Jarvinen, H., Joutel, A., Viitanen, M., Baumann, M., & Kalimo, H. (2009). Congruence between NOTCH3 mutations and GOM in 131 CADASIL patients. *Brain, 132*(Pt 4), 933–939. https://doi.org/10.1093/brain/awn364

Tournier-Lasserve, E., Joutel, A., Melki, J., Weissenbach, J., Lathrop, G. M., Chabriat, H., Mas, J. L., Cabanis, E. A., Baudrimont, M., Maciazek, J., Bach, M.-A., & Bousser, M.-G. (1993). Cerebral autosomal dominant arteriopathy with subcortical infarcts and leukoencephalopathy maps to chromosome 19q12. *Nature Genetics, 3*(3), 256–259. https://doi.org/10.1038/ng0393-256

van Engeland, N. C. A., Suarez Rodriguez, F., Rivero-Muller, A., Ristori, T., Duran, C. L., Stassen, O., Antfolk, D., Driessen, R. C. H., Ruohonen, S., Ruohonen, S. T., Nuutinen, S., Savontaus, E., Loerakker, S., Bayless, K. J., Sjoqvist, M., Bouten, C. V. C., Eriksson, J. E., & Sahlgren, C. M. (2019). Vimentin regulates Notch signaling strength and arterial remodeling in response to hemodynamic stress. *Science and Reports, 9*(1), 12415. https://doi.org/10.1038/s41598-019-48218-w

Vermeire, P. J., Lilina, A. V., Hashim, H. M., Dlabolova, L., Fiala, J., Beelen, S., Kukacka, Z., Harvey, J. N., Novak, P., & Strelkov, S. V. (2023). Molecular structure of soluble vimentin tetramers. *Science and Reports, 13*(1), 8841. https://doi.org/10.1038/s41598-023-34814-4

Wang, J., Zhang, L., Wu, G., Wu, J., Zhou, X., Chen, X., Niu, Y., Jiao, Y., Liu, Q., Liang, P., Shi, G., Wu, X., & Huang, J. (2024). Correction of a CADASIL point mutation using adenine base editors in hiPSCs and blood vessel organoids. *Journal of Genetics and Genomics = Yi Chuan Xue Bao, 51*(2), 197–207. https://doi.org/10.1016/j.jgg.2023.04.013

Yamamoto, Y., Kojima, K., Taura, D., Sone, M., Washida, K., Egawa, N., Kondo, T., Minakawa, E. N., Tsukita, K., Enami, T., Tomimoto, H., Mizuno, T., Kalaria, R. N., Inagaki, N., Takahashi, R., Harada-Shiba, M., Ihara, M., & Inoue, H. (2020). Human iPS cell-derived mural cells as an in vitro model of hereditary cerebral small vessel disease. *Molecular Brain, 13*(1), 38. https://doi.org/10.1186/s13041-020-00573-w

Zhang, R., Ouin, E., Grosset, L., Ighilkrim, K., Lebenberg, J., Guey, S., Francois, V., Tournier-Lasserve, E., Jouvent, E., & Chabriat, H. (2022). Elderly CADASIL patients with intact neurological status. *Journal of Stroke, 24*(3), 352–362. https://doi.org/10.5853/jos.2022.01578

Zhang, W., Zhao, X., Qi, X., Kimber, S. J., Hooper, N. M., & Wang, T. (2023). Induced pluripotent stem cell model revealed impaired neurovascular interaction in genetic small vessel disease Cerebral Autosomal Dominant Arteriopathy with Subcortical Infarcts and Leukoencephalopathy. *Frontiers in Cellular Neuroscience, 17*, 1195470. https://doi.org/10.3389/fncel.2023.1195470